Nano Research
DOI 10.1007/s12274-016-1313-5
Research Article
ISSN 1998-0124
CN 11-5974/O4

A titanium dioxide nanorod array as a high-affinity nano-bio interface of a microfluidic device for efficient capture of circulating tumor cells

Jichuan Qiu[1,2,§], Kun Zhao[1,§], Linlin Li[1,§], Xin Yu[1], Weibo Guo[1], Shu Wang[1], Xiaodi Zhang[1], Caofeng Pan[1] (✉), Zhong Lin Wang[1] (✉), and Hong Liu[2] (✉)

[1] *Beijing Institute of Nanoenergy and Nanosystems, Chinese Academy of Sciences; National Center for Nanoscience and Technology (NCNST), Beijing 100083, China*
[2] *Bio-Micro-Nano Functional Materials Center, State Key Laboratory of Crystal Materials, Shandong University, Jinan 250100, China*
[§] *These authors contributed equally to this work.*

Received: 5 August 2016
Revised: 23 September 2016
Accepted: 1 October 2016

KEYWORDS
TiO_2 nanorod array, circulating tumor cell, microfluidic device, nano-bio interface, 3D hierarchical structure

ABSTRACT

Nanomaterials show promising opportunities to address clinical problems (such as insufficient capture of circulating tumor cells; CTCs) via the high surface area-to-volume ratio and high affinity for biological cells. However, how to apply these nanomaterials as a nano-bio interface in a microfluidic device for efficient CTC capture with high specificity remains a challenge. In the present work, we first found that a titanium dioxide (TiO_2) nanorod array that can be conveniently prepared on multiple kinds of substrates has high affinity for tumor cells. Then, the TiO_2 nanorod array was vertically grown on the surface of a microchannel with hexagonally patterned Si micropillars via a hydrothermal reaction, forming a new kind of a micro-nano 3D hierarchically structured microfluidic device. The vertically grown TiO_2 nanorod array was used as a sensitive nano-bio interface of this 3D hierarchically structured microfluidic device, which showed high efficiency of CTC capture (76.7% ± 7.1%) in an artificial whole-blood sample.

1 Introduction

Tumor metastasis represents the most dangerous characteristic of cancer and causes 90% of cancer-related deaths [1, 2]. Metastasis in the body represents the dissemination of circulating tumor cells (CTCs) that are shed by the primary tumor site, circulate in the bloodstream, and move to secondary loci ultimately developing into metastases [3, 4]. CTCs were found even at the early stage of tumor development [5]. Because CTCs carry important information about the primary tumor, capture and identification of CTCs will provide an effective and noninvasive method for early cancer diagnosis and treatment. Nonetheless,

Address correspondence to Hong Liu, hongliu@sdu.edu.cn; Caofeng Pan, cfpan@binn.cas.cn; Zhong Lin Wang, zlwang@binn.cas.cn

effective CTC capture is still a great challenge because of the extremely low abundance of CTCs in the bloodstream.

Various technologies and devices, such as the immunomagnetic separation technology [6–9], flow cytometry [10], filter-based approaches [11, 12], and microfluidic devices [13–17], have been developed in the past decades for CTC capture and identification. The CellSearch system, which involves immunomagnetic beads conjugated with capture agents (such as an antibody against the tumor cell marker epithelial cell adhesion molecule [anti-EpCAM antibody]) for isolating CTCs, has been used in the clinic and is still the only method approved by the US Food and Drug Administration (FDA) for CTC detection in metastatic breast cancer [6, 7]. A microfluidic device has better sensitivity and efficiency of capture of CTCs because of its enhanced cell-substrate contact frequency and adjustable features [15, 18–20]. Another advantage of a microfluidic device is its low cost and low sample usage in established techniques [18]. Thus, a microfluidic device is considered one of the most promising methods for clinical capture of CTCs. However, considering the rarity of CTCs, the sensitivity and capture efficiency still need to be optimized for a microfluidic device [21].

Nanomaterials hold promise for addressing the problems of insufficient capture efficiency and low specificity via their high surface area-to-volume ratio and high affinity for biological cells [15, 21–23]. As a matter of fact, cells may encounter various nanoscale and microscale features displayed by cellular surface components and the extracellular matrix *in vivo* [24]. Some reports have shown that nanostructures at the cell–substrate interface play important roles in cellular attachment, migration, elongation, and differentiation [25–27]. Attempts to use surface nanostructures of carbon nanotubes [28], graphene oxide [29–33], Si nanowires [34], TiO_2 nanofibers [35], soft polystyrene nanotubes [36], chitosan nanofibers [37, 38], and magnetic nanoparticles [28, 39] have yielded exciting results on sensitive and effective capture of CTCs as compared to traditional methods. Among these new approaches, TiO_2 nanomaterials have received more attention because of their good biocompatibility, high affinity for cells, and easy fabrication with diverse morphologies [35, 40–43]. For example, Zhang et al. demonstrated that electrospun TiO_2 nanofiber has good affinity for CTCs, and a TiO_2 nanofiber-coated substrate has high capture efficiency as compared to that without TiO_2 nanofiber [35]. Meng et al. developed a photoresponsive self-cleaning TiO_2 nanosisal-like surface coating for CTC capture [40]. Given the advantages of microfluidics and nanostructural interfaces, we can hypothesize that the use of nanomaterials as a cell–device interface in a microfluidic device can combine the advantages of a microfluidic device and nanomaterials.

In our previous study, we found that a rutile TiO_2 nanorod array can be easily grown on various substrates by a hydrothermal method and that it facilitates the adhesion and prolonged culture of mesenchymal stem cells (MSCs) [44]. Considering the good biocompatibility, high cell affinity, and the large surface area for antibody modification of a TiO_2 nanorod array, herein, we used the surface of a TiO_2 nanorod array to improve the affinity, capture, identification, and prolonged culture of CTCs. Furthermore, a TiO_2 nanorod array was applied as a nano-bio interface of a micro-nano 3D hierarchically structured microfluidic device with hexagonally patterned Si pillars in channels. This newly designed micro-nano 3D hierarchically structured microfluidic device possesses high efficiency of capture of CTCs and thus represents a new technique for CTC-based cancer diagnosis with high sensitivity and reliability.

2 Results and discussion

The TiO_2 nanorod array was synthesized on a Si substrate after vacuum sputtering of a TiO_2 seed layer, followed by hydrothermal growth of a TiO_2 nanorod (Fig. 1(a)). The nanorod array vertically grown on the Si substrate (Fig. 1(b)) was examined from the top view and cross-sectional view by scanning electron microscopy (SEM) (Fig. 1(c)). The individual TiO_2 nanorods were approximately 1.5 μm in length and 80 nm in diameter (Fig. 1(c)). The density of TiO_2 nanorods was calculated (~35 rods per μm^2) by counting the nanorods in an SEM image. The growth direction of TiO_2 nanorods was along [001], as depicted in the high-resolution transmission electron microscopy (TEM) images in Fig. 1(d). The high surface area-to-

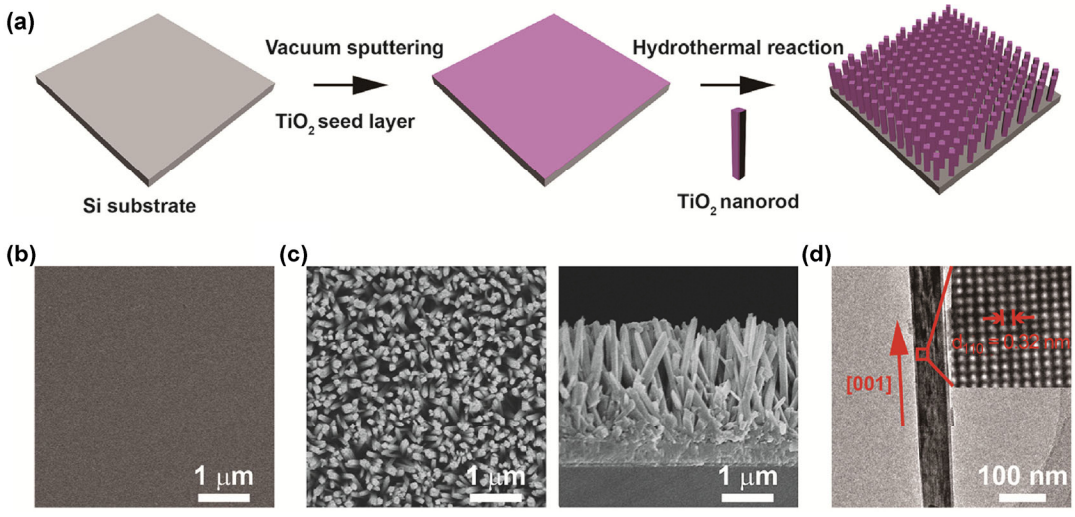

Figure 1 A TiO_2 nanorod array on a Si substrate. (a) A scheme showing the synthesis of a TiO_2 nanorod array on a Si substrate. (b) An SEM image of the Si substrate. (c) SEM images showing the top view and side view of the TiO_2 nanorod array on Si. (d) A TEM image of a single TiO_2 nanorod and high-resolution TEM images of the selected area (inset).

volume ratio of the vertically grown TiO_2 nanorod array should provide more antibody modification sites for specific cell attachment as compared with a smooth Si substrate.

The TiO_2 nanorod array was functionalized with a tumor cell-specific (anti-EpCAM) antibody for tumor cell recognition and capture (Fig. 2(a)). To be precise, after 3-mercaptopropyl trimethoxysilane (MPTMS) modification, a layer of streptavidin (SA) was applied to the TiO_2 nanorod array by means of a coupling agent, N-maleimidobutyryloxy succinimide ester (GMBS), which reacted with a –SH group of MPTMS and an $–NH_2$ group of SA. Then, the biotinylated anti-EpCAM antibody was freshly conjugated with the streptavidin-coated substrates for specific CTC capture. To evaluate the cell capture performance of the TiO_2 nanorod array compared to the Si substrate, a human breast cancer cell line (MCF-7) with strong expression of EpCAM was used as target cells. The cells were added into a serum-free culture medium to a final concentration of 10^5 per mL and flowed through the substrate (1 cm × 1 cm) in a circulation chamber by the action of a microinjection pump at a flow rate of 1 $mL \cdot h^{-1}$ for 1 h (Fig. S1 in the Electronic Supplementary Material (ESM)). The cytoskeleton and nuclei of the captured cells were stained green and blue, respectively, by fluorescein isothiocyanate conjugated phalloidin (FITC-phalloidin) and 4′,6-diamidino-2-phenylindole (DAPI), respectively. As shown in Fig. 2(b), the biotinylated anti-EpCAM antibody-modified substrate with a TiO_2 nanorod array captured much more target cells, whereas the Si substrate with or without modification by the biotinylated anti-EpCAM antibody captured few cells. Even without the modification by the anti-EpCAM antibody, the TiO_2 nanorod array showed greater cell capture ability than the anti-EpCAM antibody-modified Si substrate. Moreover, target cells captured on the TiO_2 nanorod array appeared spread and had more pseudopodia attached to the nanorods, whereas the cells captured by the Si substrate showed spherical morphology with few extended pseudopodia (Fig. 2(c)). These results suggested that the TiO_2 nanorod array improved the contact and adhesion ability of the cells toward the substrates, as a result of the strong cell–TiO_2 nanorod array affinity and interaction. To further evaluate the selective ability of the TiO_2 nanorod array to capture target cells, a nonspecific cell line (HeLa cells) with low EpCAM expression was also flowed through the TiO_2 nanorod array under the same conditions. The results indicated that only a few HeLa cells were captured by the TiO_2 nanorod array as compared to MCF-7 cells; this finding is suggestive of good specificity for target cells (Fig. 2(d)).

Then, the TiO_2 nanorod array was assembled in a microfluidic device as a nanostructure cell–device

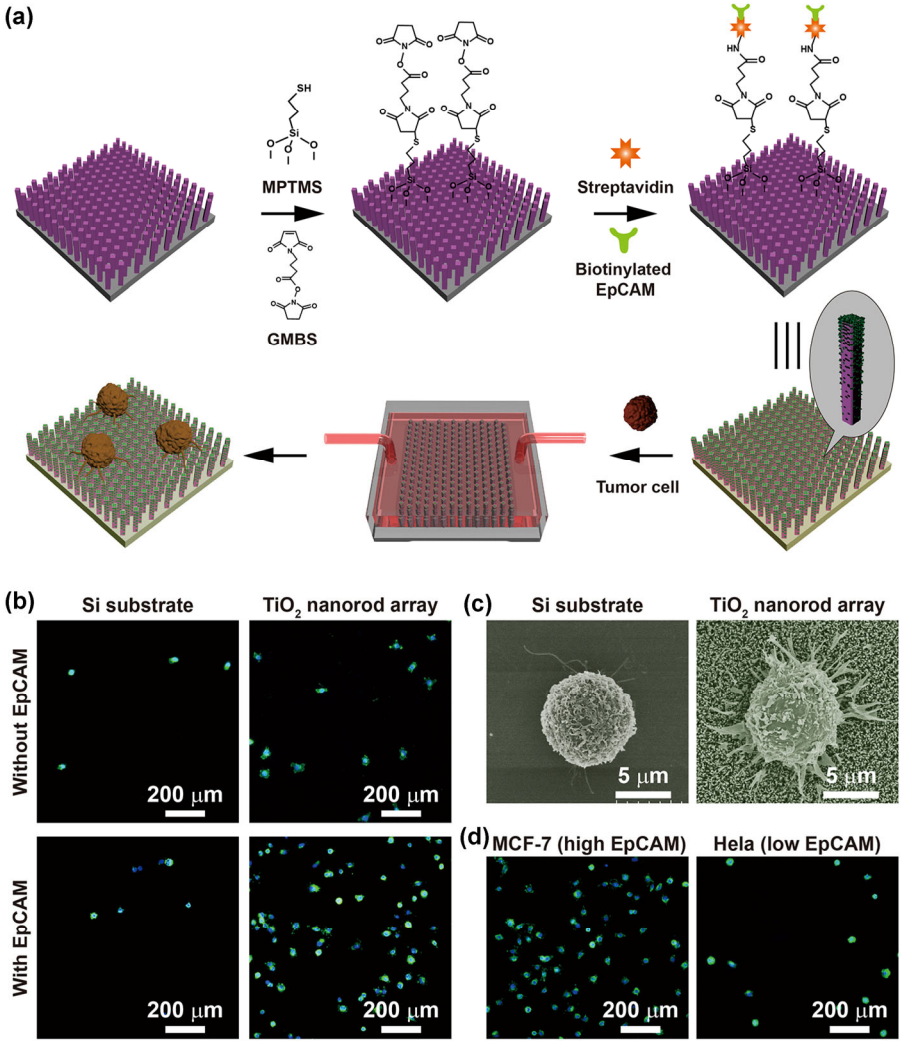

Figure 2 The planar surface of a TiO_2 nanorod array for capture of MCF-7 cells. (a) A scheme showing the modification of the TiO_2 nanorod array with an antibody for tumor cell capture. (b) The capture ability of a Si substrate and TiO_2 nanorod array (toward MCF-7 cells) with or without EpCAM modification. The cytoskeleton and nuclei were stained green and blue, respectively. (c) SEM images of target cells captured by the Si substrate with and without the TiO_2 nanorod array. (d) Selective affinity of the TiO_2 nanorod array for MCF-7 cells (high EpCAM expression) and HeLa cells (low EpCAM expression). The cytoskeleton and nuclei were stained green and blue, respectively.

interface for improvement of CTC capture. The microfluidic device was composed of a 40 mm × 20 mm Si substrate, on which there was a microfluidic channel of 70 mm in length, 4 mm in width, and 115 μm in height (Fig. 3(a)). To improve the cell–device contact frequency, 2.8×10^5 hexagonally patterned Si micropillars were constructed in the microfluidic channel (Fig. 3(a)). The whole surface of the microfluidic channel, including the side wall of the Si pillars and the bottom of the channel, was coated with a layer of a vertically grown TiO_2 nanorod array, forming a micro-nano 3D hierarchical structure. As shown in Fig. 3(b), the silicon substrates were first coated with a layer of a photoresist, which had patterned pitch prepared by photolithography (PL), and the microchannel with Si micropillars was constructed after a plasma etching process. After removal of the photoresist with acetone, the substrate was vacuum-spurred with a layer of a TiO_2 seed, and the TiO_2 nanorod array was hydrothermally grown on it. Next, the micro-nano 3D hierarchically structured microfluidic device was constructed after the substrate was encapsulated by

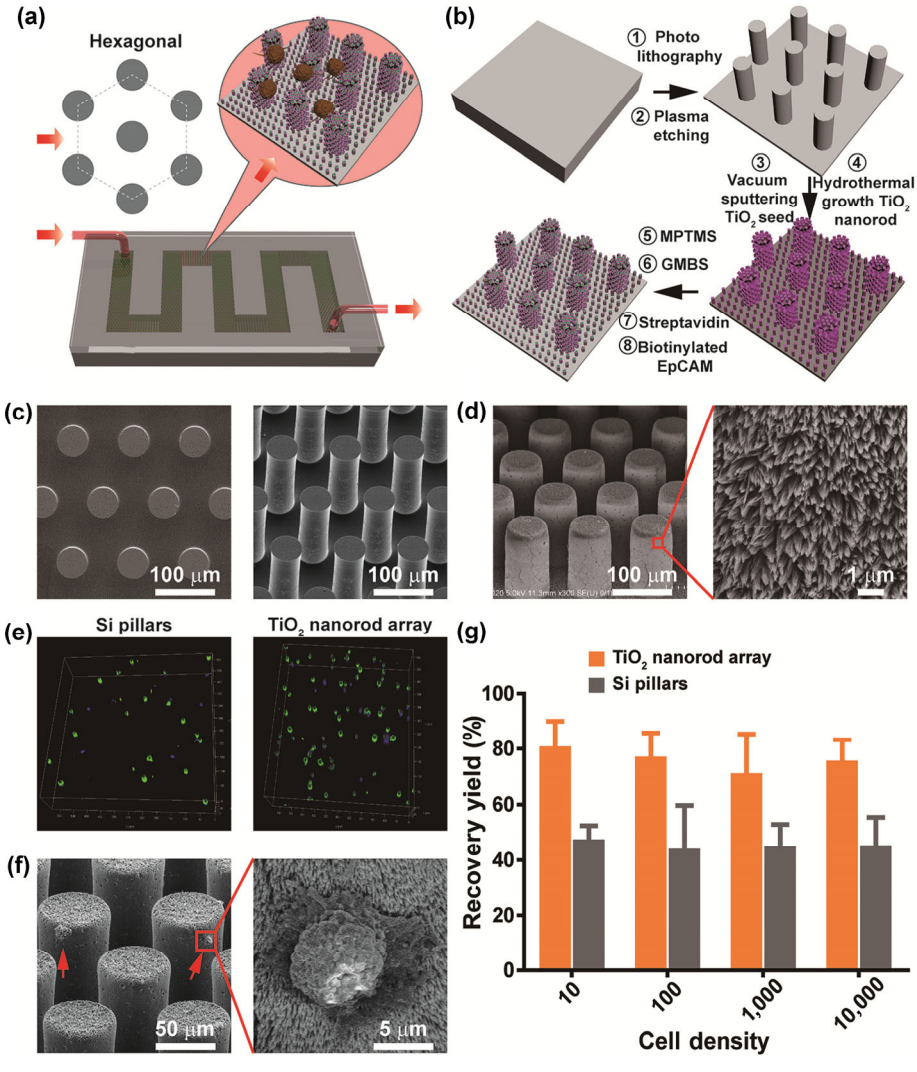

Figure 3 The TiO_2 nanorod array as a cell–substrate interface in a microfluidic device for improved tumor cell capture. (a) A scheme of the microfluidic device for tumor cell capture. (b) A scheme showing the preparation of a TiO_2 nanorod array-modified microfluidic device. (c) SEM images (top and side view) of hexagonally patterned Si pillars in the microfluidic device. (d) SEM images of TiO_2 nanorod array-modified Si pillars. (e) The capture ability of the microfluidic device toward MCF-7 cells with or without the TiO_2 nanorod array modification. (f) SEM images of target cells captured by the TiO_2 nanorod array-modified Si pillars. (g) Capture efficiency of the microfluidic device toward MCF-7 cells with or without the TiO_2 nanorod array modification ($n = 3$).

polydimethylsiloxane (PDMS) with two holes as the entrance and the exit, forming a microfluidic device. The device was functionalized with the anti-EpCAM antibody by sequential flowing of MPTMS, GMBS, streptavidin, and the biotinylated anti-EpCAM antibody. As shown in Fig. 3(c), the hexagonally patterned Si micropillars in the resulting microchannel had a dimeter of ~50 μm, and the distance between Si pillars was also ~50 μm. The height of the channel and Si pillars was ~115 μm (Fig. S2 in the ESM). After the hydrothermal reaction, a layer of a TiO_2 nanorod array was vertically grown on all the side walls of the Si pillars (Fig. 3(d) and Fig. S3 in the ESM), whose diameter, height, and interspacing were similar to those of the TiO_2 nanorod array grown on the plain Si substrate.

After the modification with the anti-EpCAM antibody, we flowed 1 mL of an MCF-7 cell suspension (10,000 per mL) through the microfluidic device at a flow rate of 0.5 $mL \cdot h^{-1}$ at 37 °C (Fig. S4 in the ESM). As shown in confocal laser scanning microscopy (CLSM)

images (Fig. 3(e)), the microfluidic device with the TiO_2 nanorod array as a nano-bio interface captured more target cells, whereas the microfluidic device without the TiO_2 nanorod array captured fewer cells. Moreover, after flowing through the micro-nano 3D hierarchically structured microfluidic device, the cells adhered tightly to the surface of the TiO_2 nanorod array grown on the side wall of the Si pillars (Fig. 3(f)). Additionally, most target cells captured by the microfluidic device without the TiO_2 nanorod array were located at the bottom of the microfluidic channel, whereas target cells captured by the microfluidic device with the surface layer of the TiO_2 nanorod array were distributed not only on the bottom of the channel but also on the side wall of the Si micropillars (Fig. S5 in the ESM). Four cell concentrations were used for evaluating the capture efficiency of the micro-nano 3D hierarchically structured microfluidic device. The capture yield of the microfluidic device was calculated by counting of the fluorescently labeled target cells under CLSM. As shown in Fig. 3(g), after flowing of cell suspensions of different concentrations, the capture yield of the microfluidic device with the surface layer of the TiO_2 nanorod array was calculated and found to be 80.0% ± 10.0%, 76.3% ± 9.5%, 70.3% ± 15.0%, and 74.9% ± 8.5% (n = 3) at tumor cell density 10, 100, 1,000, and 10,000, respectively. These data were apparently better than the capture yield of the microfluidic device without the TiO_2 nanorod array (46.7% ± 5.8%, 43.3% ± 16.3%, 44.0% ± 8.9%, and 44.6% ± 10.9% (n = 3) at the cell density of 10, 100, 1,000, and 10,000, respectively). These results revealed that the TiO_2 nanorod array containing the immobilized anti-EpCAM antibody was sufficiently sensitive for the capture of tumor cells. As a bio-nano interface of the microfluidic device, the TiO_2 nanorod array improved the ability to capture tumor cells significantly and effectively.

To demonstrate the potential clinical applications of the micro-nano 3D hierarchically structured microfluidic device, artificial whole-blood samples containing CTCs were prepared to evaluate the CTC capture ability of the microfluidic device containing the TiO_2 nanorod array (Fig. 4(a)). Artificial CTC blood samples were prepared by spiking normal human blood with MCF-7 cells at cell density ~10, 50, or 100 cells·mL^{-1}. After we flowed the blood samples through the TiO_2 nanorod array-modified microfluidic device, the captured cells were stained with an Alexa Fluor 488-conjugated anti-CD45 antibody (CD45 is a marker of white blood cells; WBCs), an Alexa Fluor 647-conjugated anticytokeratin antibody (cytokeratin is a protein marker of epithelial cells), and with DAPI (nuclear staining) to identify and count CTCs among nonspecifically captured WBCs. The latter were identified as DAPI- and CD45-positive, whereas CTCs were identified as positive for DAPI and cytokeratin but negative for CD45 (Fig. 4(b)). The CTC recovery rates from whole-blood samples were 76.7% ± 7.1%, 69.3% ± 13.4%, and 68% ± 11.3% (n = 3) when the tumor cell density in whole blood was 10, 50, and 100 per mL, respectively (Fig. 4(c)). After capture in the TiO_2 nanorod array-modified microfluidic device, MCF-7 cells were cultured in the microchannel for 7 days. The captured cells grew and proliferated well in the microchannel with the layer of the TiO_2 nanorod array (Fig. 4(d)), suggesting that a TiO_2 nanorod array can be used as a biocompatible cell–substrate interface for prolonged culture and proliferation of CTCs. For patients with very low abundance of CTCs in systemic circulation, the proliferation of CTCs directly after cell capture makes gene or protein analysis possible for cancer diagnosis (as a "liquid biopsy") and for subsequent personalized treatment.

3 Conclusions

In the present work, we demonstrated that a vertically grown TiO_2 nanorod array has high affinity for tumor cells and better efficiency of capture of tumor cells in comparison with a smooth Si substrate. Taking advantage of the facile preparation of a TiO_2 nanorod array on the surface of various kinds of substrates, we constructed a novel micro-nano 3D hierarchically structured microfluidic device using the TiO_2 nanorod array as a sensitive nano-bio interface for effective capture of CTCs. The micro-nano 3D hierarchically structured microfluidic device shows high efficiency of CTC capture (76.7% ± 7.1%) in artificial whole-blood samples. Although further work is needed to refine the conditions for clinical capture of CTCs, the potential practical applications such as isolation of

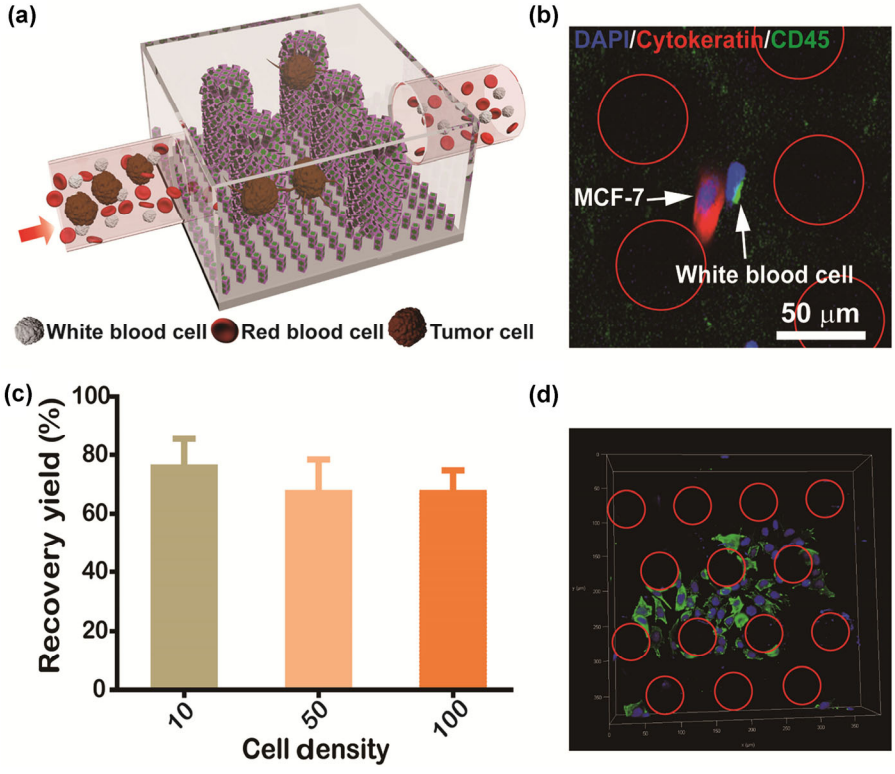

Figure 4 The microfluidic device involving the TiO_2 nanorod array as a cell–substrate interface for capturing tumor cells in whole blood. (a) A schematic model of a microfluidic device for tumor cell capture in whole blood. (b) Immunostaining of MCF-7 cells and white blood cells for nuclei (DAPI, blue), for cytokeratin (red), and for CD45 (green). Red circles indicate Si micropillars. (c) Capture efficiency of the TiO_2 nanorod array-modified microfluidic device toward MCF-7 cells in a whole-blood sample (n = 3). (d) A fluorescence microscopy image of MCF-7 cells cultured for 1 week (green: cytoskeleton, blue: nuclei) captured by a TiO_2 nanorod array-modified microfluidic device from whole blood. Red circles indicate Si micropillars.

rare populations of cells, early diagnosis and long-term monitoring of cancer, and molecular biological analysis of captured rare cells are worth the effort.

Acknowledgements

The authors are thankful for funding from the National Natural Science Foundation of China (Nos. 51402063, 51432005, 61405040, 61505010, 51502018, 31270022, and 81471784), the "100 Talents Program" of the Chinese Academy of Sciences, Beijing City Committee of science and technology (No. Z151100003315010), Beijing Natural Science Foundation (Nos. 2164077 and 2164076), the Fundamental Research Funds of Shandong University (No. 2014QY003), and the Youth Innovation Promotion Association of the Chinese Academy of Sciences (No. 2015023). The authors also acknowledge the support from the "thousands talents" program for pioneer researchers and his innovation team, and support from the President Funding of the Chinese Academy of Sciences.

Electronic Supplementary Material: Supplementary material (experimental section and detailed images of as prepared 3D hierarchical structured microfluidic device) is available in the online version of this article at http://dx.doi.org/10.1007/s12274-016-1313-5.

References

[1] Gupta, G. P.; Massagué, J. Cancer metastasis: Building a framework. *Cell* **2006**, *127*, 679–695.

[2] Weigelt, B.; Peterse, J. L.; Van't Veer, L. J. Breast cancer metastasis: Markers and models. *Nat. Rev. Cancer* **2005**, *5*, 591–602.

[3] Chambers, A. F.; Groom, A. C.; MacDonald, I. C. Metastasis: Dissemination and growth of cancer cells in metastatic sites. *Nat. Rev. Cancer* **2002**, *2*, 563–572.

[4] Fidler, I. J. The pathogenesis of cancer metastasis: The 'seed and soil' hypothesis revisited. *Nat. Rev. Cancer* **2003**, *3*, 453–458.

[5] Nakagawa, T.; Martinez, S. R.; Goto, Y.; Koyanagi, K.; Kitago, M.; Shingai, T.; Elashoff, D. A.; Ye, X.; Singer, F. R.; Giuliano, A. E. Detection of circulating tumor cells in early-stage breast cancer metastasis to axillary lymph nodes. *Clin. Cancer Res.* **2007**, *13*, 4105–4110.

[6] Cristofanilli, M.; Budd, G. T.; Ellis, M. J.; Stopeck, A.; Matera, J.; Miller, M. C.; Reuben, J. M.; Doyle, G. V.; Allard, W. J.; Terstappen, L. W. M. M. et al. Circulating tumor cells, disease progression, and survival in metastatic breast cancer. *N. Engl. J. Med.* **2004**, *351*, 781–791.

[7] Shaffer, D. R.; Leversha, M. A.; Danila, D. C.; Lin, O.; Gonzalez-Espinoza, R.; Gu, B.; Anand, A.; Smith, K.; Maslak, P.; Doyle, G. V. et al. Circulating tumor cell analysis in patients with progressive castration-resistant prostate cancer. *Clin. Cancer Res.* **2007**, *13*, 2023–2029.

[8] Lu, N. N.; Xie, M.; Wang, J.; Lv, S. W.; Yi, J. S.; Dong, W. G.; Huang, W. H. Biotin-triggered decomposable immunomagnetic beads for capture and release of circulating tumor cells. *ACS Appl. Mater. Interfaces* **2015**, *7*, 8817–8826.

[9] Fang, S.; Wang, C.; Xiang, J.; Cheng, L.; Song, X. J.; Xu, L. G.; Peng, R.; Liu, Z. Aptamer-conjugated upconversion nanoprobes assisted by magnetic separation for effective isolation and sensitive detection of circulating tumor cells. *Nano Res.* **2014**, *7*, 1327–1336.

[10] He, W.; Wang, H. F.; Hartmann, L. C.; Cheng, J.-X.; Low, P. S. *In vivo* quantitation of rare circulating tumor cells by multiphoton intravital flow cytometry. *Proc. Natl. Acad. Sci. USA* **2007**, *104*, 11760–11765.

[11] Lecharpentier, A.; Vielh, P.; Perez-Moreno, P.; Planchard, D.; Soria, J. C.; Farace, F. Detection of circulating tumour cells with a hybrid (epithelial/mesenchymal) phenotype in patients with metastatic non-small cell lung cancer. *Br. J. Cancer* **2011**, *105*, 1338–1341.

[12] Tan, S. J.; Yobas, L.; Lee, G. Y. H.; Ong, C. N.; Lim, C. T. Microdevice for the isolation and enumeration of cancer cells from blood. *Biomed. Microdevices* **2009**, *11*, 883–892.

[13] Adams, A. A.; Okagbare, P. I.; Feng, J.; Hupert, M. L.; Patterson, D.; Göttert, J.; McCarley, R. L.; Nikitopoulos, D.; Murphy, M. C.; Soper, S. A. Highly efficient circulating tumor cell isolation from whole blood and label-free enumeration using polymer-based microfluidics with an integrated conductivity sensor. *J. Am. Chem. Soc.* **2008**, *130*, 8633–8641.

[14] Nagrath, S.; Sequist, L. V.; Maheswaran, S.; Bell, D. W.; Irimia, D.; Ulkus, L.; Smith, M. R.; Kwak, E. L.; Digumarthy, S.; Muzikansky, A. et al. Isolation of rare circulating tumour cells in cancer patients by microchip technology. *Nature* **2007**, *450*, 1235–1239.

[15] Lin, M.; Chen, J.-F.; Lu, Y.-T.; Zhang, Y.; Song, J. Z.; Hou, S.; Ke, Z. F.; Tseng, H.-R. Nanostructure embedded microchips for detection, isolation, and characterization of circulating tumor cells. *Acc. Chem. Res.* **2014**, *47*, 2941–2950.

[16] Sarioglu, A. F.; Aceto, N.; Kojic, N.; Donaldson, M. C.; Zeinali, M.; Hamza, B.; Engstrom, A.; Zhu, H. L.; Sundaresan, T. K.; Miyamoto, D. T. et al. A microfluidic device for label-free, physical capture of circulating tumor cell clusters. *Nat. Methods* **2015**, *12*, 685–691.

[17] Yu, X. L.; Wang, B. R.; Zhang, N. G.; Yin, C. Q.; Chen, H.; Zhang, L. L.; Cai, B.; He, Z. B.; Rao, L.; Liu, W. et al. Capture and release of cancer cells by combining on-chip purification and off-chip enzymatic treatment. *ACS App. Mater. Interfaces* **2015**, *7*, 24001–24007.

[18] Whitesides, G. M. The origins and the future of microfluidics. *Nature* **2006**, *442*, 368–373.

[19] Stott, S. L.; Hsu, C.-H.; Tsukrov, D. I.; Yu, M.; Miyamoto, D. T.; Waltman, B. A.; Rothenberg, S. M.; Shah, A. M.; Smas, M. E.; Korir, G. K. et al. Isolation of circulating tumor cells using a microvortex-generating herringbone-chip. *Proc. Natl. Acad. Sci. USA* **2010**, *107*, 18392–18397.

[20] Murlidhar, V.; Zeinali, M.; Grabauskiene, S.; Ghannad-Rezaie, M.; Wicha, M. S.; Simeone, D. M.; Ramnath, N.; Reddy, R. M.; Nagrath, S. A radial flow microfluidic device for ultra-high-throughput affinity-based isolation of circulating tumor cells. *Small* **2014**, *10*, 4895–4904.

[21] Yoon, H. J.; Kozminsky, M.; Nagrath, S. Emerging role of nanomaterials in circulating tumor cell isolation and analysis. *ACS Nano* **2014**, *8*, 1995–2017.

[22] Wang, L. X.; Asghar, W.; Demirci, U.; Wan, Y. Nano-structured substrates for isolation of circulating tumor cells. *Nano Today* **2013**, *8*, 374–387.

[23] Li, Y. Q.; Chandran, B. K.; Lim, C. T.; Chen, X. D. Rational design of materials interface for efficient capture of circulating tumor cells. *Adv. Sci.* **2015**, *2*, DOI: 10.1002/advs.201500118.

[24] Dvir, T.; Timko, B. P.; Kohane, D. S.; Langer, R. Nano-technological strategies for engineering complex tissues. *Nat. Nanotechnol.* **2011**, *6*, 13–22.

[25] Dang, J. M.; Leong, K. W. Myogenic induction of aligned mesenchymal stem cell sheets by culture on thermally responsive electrospun nanofibers. *Adv. Mater.* **2007**, *19*, 2775–2779.

[26] Stevens, M. M.; George, J. H. Exploring and engineering the cell surface interface. *Science* **2005**, *310*, 1135–1138.

[27] Yang, M. T.; Sniadecki, N. J.; Chen, C. S. Geometric considerations of micro- to nanoscale elastomeric post arrays to study cellular traction forces. *Adv. Mater.* **2007**, *19*, 3119–3123.

[28] Wu, C.-H.; Huang, Y.-Y.; Chen, P.; Hoshino, K.; Liu, H. Y.; Frenkel, E. P.; Zhang, J. X.; Sokolov, K. V. Versatile immunomagnetic nanocarrier platform for capturing cancer cells. *ACS Nano* **2013**, *7*, 8816–8823.

[29] Li, Y. Y.; Lu, Q. H.; Liu, H. L.; Wang, J. F.; Zhang, P. C.; Liang, H. G.; Jiang, L.; Wang, S. T. Antibody-modified reduced graphene oxide films with extreme sensitivity to circulating tumor cells. *Adv. Mater.* **2015**, *27*, 6848–6854.

[30] Yoon, H. J.; Kim, T. H.; Zhang, Z.; Azizi, E.; Pham, T. M.; Paoletti, C.; Lin, J.; Ramnath, N.; Wicha, M. S.; Hayes, D. F. et al. Sensitive capture of circulating tumour cells by functionalized graphene oxide nanosheets. *Nat. Nanotechnol.* **2013**, *8*, 735–741.

[31] Li, W.; Wang, J. S.; Ren, J. S.; Qu, X. G. 3D graphene oxide–polymer hydrogel: Near-infrared light-triggered active scaffold for reversible cell capture and on-demand release. *Adv. Mater.* **2013**, *25*, 6737–6743.

[32] Yoon, H. J.; Shanker, A.; Wang, Y.; Kozminsky, M.; Jin, Q.; Palanisamy, N.; Burness, M. L.; Azizi, E.; Simeone, D. M.; Wicha, M. S. et al. Tunable thermal-sensitive polymer-graphene oxide composite for efficient capture and release of viable circulating tumor cells. *Adv. Mater.* **2016**, *28*, 4891–4897.

[33] Yin, S. Y.; Wu, Y. L.; Hu, B. H.; Wang, Y.; Cai, P. Q.; Tan, C. K.; Qi, D. P.; Zheng, L. Y.; Leow, W. R.; Tan, N. S. et al. Three-dimensional graphene composite macroscopic structures for capture of cancer cells. *Adv. Mater. Interfaces* **2014**, *1*, DOI: 10.1002/admi.201300043.

[34] Wang, S. T.; Wang, H.; Jiao, J.; Chen, K. J.; Owens, G. E.; Kamei, K. I.; Sun, J.; Sherman, D. J.; Behrenbruch, C. P.; Wu, H. et al. Three-dimensional nanostructured substrates toward efficient capture of circulating tumor cells. *Angew. Chem.* **2009**, *121*, 9132–9135.

[35] Zhang, N. G.; Deng, Y. L.; Tai, Q. D.; Cheng, B. R.; Zhao, L. B.; Shen, Q. L.; He, R. X.; Hong, L. Y.; Liu, W.; Guo, S. S. et al. Electrospun TiO_2 nanofiber-based cell capture assay for detecting circulating tumor cells from colorectal and gastric cancer patients. *Adv. Mater.* **2012**, *24*, 2756–2760.

[36] Liu, X. L.; Chen, L.; Liu, H. L.; Yang, G.; Zhang, P. C.; Han, D.; Wang, S. T.; Jiang, L. Bio-inspired soft polystyrene nanotube substrate for rapid and highly efficient breast cancer-cell capture. *NPG Asia Mater.* **2013**, *5*, e63.

[37] Sun, N.; Wang, J.; Ji, L. Y.; Hong, S. N.; Dong, J. J.; Guo, Y. H.; Zhang, K. C.; Pei, R. J. A cellular compatible chitosan nanoparticle surface for isolation and *in situ* culture of rare number ctcs. *Small* **2015**, *11*, 5444–5451.

[38] Sun, N.; Liu, M.; Wang, J.; Wang, Z. L.; Li, X. P.; Jiang, B.; Pei, R. J. Chitosan nanofibers for specific capture and nondestructive release of CTCs assisted by pCBMA brushes. *Small* **2016**, *12*, 5090–5097.

[39] Hoshino, K.; Huang, Y.-Y.; Lane, N.; Huebschman, M.; Uhr, J. W.; Frenkel, E. P.; Zhang, X. J. Microchip-based immunomagnetic detection of circulating tumor cells. *Lab Chip* **2011**, *11*, 3449–3457.

[40] Meng, J. X.; Zhang, P. C.; Zhang, F. L.; Liu, H. L.; Fan, J. B.; Liu, X. L.; Yang, G.; Jiang, L.; Wang, S. T. A self-cleaning TiO_2 nanosisal-like coating toward disposing nanobiochips of cancer detection. *ACS Nano* **2015**, *9*, 9284–9291.

[41] He, R. X.; Zhao, L. B.; Liu, Y. M.; Zhang, N. G.; Cheng, B. R.; He, Z. B.; Cai, B.; Li, S. Z.; Liu, W.; Guo, S. S. et al. Biocompatible TiO_2 nanoparticle-based cell immunoassay for circulating tumor cells capture and identification from cancer patients. *Biomed. Microdevices* **2013**, *15*, 617–626.

[42] Wu, S. L.; Weng, Z. Y.; Liu, X. M.; Yeung, K. W. K.; Chu, P. K. Functionalized TiO_2 based nanomaterials for biomedical applications. *Adv. Funct. Mater.* **2014**, *24*, 5464–5481.

[43] Sun, N.; Li, X.; Wang, Z.; Zhang, R.; Wang, J.; Wang, K.; Pei, R. A multiscale TiO_2 nanorod array for ultrasensitive capture of circulating tumor cells. *ACS Appl. Mater. Interfaces* **2016**, *8*, 12638–12343.

[44] Qiu, J. C.; Li, J. H.; Wang, S.; Ma, B. J.; Zhang, S.; Guo, W. B.; Zhang, X. D.; Wei, T.; Sang, Y. H.; Liu, H. TiO_2 nanorod array constructed nanotopography for regulation of mesenchymal stem cells fate and the realization of location-committed stem cell differentiation. *Small* **2016**, *12*, 1770–1778.